Frequent POLE-driven hypermutation in ovarian endometrioid cancer revealed by mutational signatures in RNA sequencing

Jaime I. Davila[1,2]*, Pritha Chanana[3], Vivekananda Sarangi[2], Zachary C. Fogarty[2], S. John Weroha[4], Ruifeng Guo[5], Ellen L. Goode[2], Yajue Huang[5] and Chen Wang[2]*

Abstract

Background: DNA polymerase epsilon (POLE) is encoded by the POLE gene, and *POLE*-driven tumors are characterized by high mutational rates. *POLE*-driven tumors are relatively common in endometrial and colorectal cancer, and their presence is increasingly recognized in ovarian cancer (OC) of endometrioid type. *POLE*-driven cases possess an abundance of TCT > TAT and TCG > TTG somatic mutations characterized by mutational signature 10 from the Catalog of Somatic Mutations in Cancer (COSMIC). By quantifying the contribution of COSMIC mutational signature 10 in RNA sequencing (RNA-seq) we set out to identify *POLE*-driven tumors in a set of unselected Mayo Clinic OC.

Methods: Mutational profiles were calculated using expressed single-nucleotide variants (eSNV) in the Mayo Clinic OC tumors (n = 195), The Cancer Genome Atlas (TCGA) OC tumors (n = 419), and the Genotype-Tissue Expression (GTEx) normal ovarian tissues (n = 84). Non-negative Matrix Factorization (NMF) of the mutational profiles inferred the contribution per sample of four distinct mutational signatures, one of which corresponds to COSMIC mutational signature 10.

Results: In the Mayo Clinic OC cohort we identified six tumors with a predicted contribution from COSMIC mutational signature 10 of over five mutations per megabase. These six cases harbored known POLE hotspot mutations (*P286R*, *S297F*, *V411L*, and *A456P*) and were of endometrioid histotype (*P* = 5e−04). These six tumors had an early onset (average age of patients at onset, 48.33 years) when compared to non-POLE endometrioid OC cohort (average age at onset, 60.13 years; *P* = .008). Samples from TCGA and GTEx had a low COSMIC signature 10 contribution (median 0.16 mutations per megabase; maximum 1.78 mutations per megabase) and carried no POLE hotspot mutations.

Conclusions: From the largest cohort of RNA-seq from endometrioid OC to date (n = 53), we identified six hypermutated samples likely driven by POLE (frequency, 11%). Our result suggests the clinical need to screen for POLE driver mutations in endometrioid OC, which can guide enrollment in immunotherapy clinical trials.

Keywords: Hypermutation, Mutational signatures, Ovarian endometrioid cancer, POLE, RNA-seq

Background

DNA polymerase epsilon (POLE) is a key member of the DNA polymerase family and is involved in error correction during replication [1]. Somatic mutations in the exonuclease domain of *POLE* have been identified in 7−12% of uterine endometrial cancers, in 1−2% of colorectal cancers, and at low frequencies in stomach cancer,

---

*Correspondence: davila3@stolaf.edu; wang.chen@mayo.edu

[1] Department of Mathematics, Statistics and Computer Science, St Olaf College, Northfield, MN, USA

[2] Department of Health Sciences Research, Mayo Clinic, Rochester, MN, USA

Full list of author information is available at the end of the article

Davila *et al. BMC Med Genomics*   (2021) 14:165

Page 2 of 6

glioblastoma, breast cancer, and others [2–5]. Recurrent hotspot mutations include *P286R*, *S297F*, and *V411L*, which are characterized by ultramutation [5, 6]. Patients with *POLE*-driven endometrial cancer have a favorable prognosis, a higher neoantigen load, an increased number of tumor-infiltrating lymphocytes, and they may benefit from immunotherapy [6–8].

Somatic *POLE* mutations are uncommon in serous ovarian cancer (OC) [9, 10] but the presence of *POLE* mutations is increasingly recognized in ovarian endometrioid cancer (OEC) [10–14]. Patients with *POLE*-driven OEC have earlier disease onset, and an increased number of *CD8+* intraepithelial tumor-infiltrating lymphocytes [11, 14]. The prevalence of *POLE*-driven tumors in different OEC studies ranges from 3 to 13% [10–12, 14–16], and is likely driven by sample size, cohort selection criteria, and type of mutation detection assay. Interestingly, in a Japanese cohort of concurrent ovarian and endometrial cancer, the frequency of *POLE* mutations was high (five of 8 cases; 62%) detected by Sanger sequencing [13]; however, the reported *POLE* mutations (*Q292E*, *E396V*, *D287N*, and *N293D*) do not correspond to known hotspot mutations. This result highlights the need to ascertain the effects of particular *POLE* mutations and whether they are accompanied by hypermutation.

POLE-driven tumors are associated with a distinct mutational signature found in whole-genome sequencing from tumor-normal pairs which is characterized by a high number of TCT > TAT and TCG > TTG mutations [4, 17]. Such distinct mutational profile is known as COSMIC mutational signature 10 [17]. Exome sequencing detected an abundance of COSMIC mutational signature 10 in OEC cases with known *POLE* hotspot mutations [16]. Previously, we developed a novel method for inferring and quantifying distinct mutational signatures using RNA sequencing (RNA-seq) data [18, 19]. We applied this method in tumor-only fresh-frozen RNA sequencing (RNA-seq) samples in endometrial cancer and colorectal cancer tumors from The Cancer Genome Atlas (TCGA) and identified *POLE* cases with high specificity and sensitivity [19].

Using previously published RNA-seq from a Mayo Clinic OC cohort (n=195), which included the largest set of OEC transcriptomes to date (n=53), we sought to leverage the mutational signatures approach to identify *POLE*-driven cases and to characterize their clinical characteristics [20, 21].

Methods
Mayo Clinic and public data selection and RNA-seq
Selected participants were patients who were at least 20 years old and were ascertained at Mayo Clinic from 1992 through 2009 within one year after receiving a

pathologically confirmed diagnosis of primary invasive epithelial OC, fallopian tube cancer, or primary peritoneal cancer. (Table 1). Patients were treated using standard first line platinum-based chemotherapy. Tumors were snap frozen immediately after surgery and stored at −80 °C. A gynecologic pathologist confirmed the clinical diagnoses and verified the tumor histology and grade and the presence of 70% tumor content before RNA extraction from fresh frozen tissue. As described previously [20, 21] transcriptomic sequencing was performed in four batches with TruSeq Library Preparation kits (Stranded Total RNA Library Preparation Kit or RNA Library Preparation Kit v2; Illumina, Inc) and sequenced on the Illumina HiSeq 2000 sequencer with 100–base pair paired-end reads. All patients gave informed consent; all protocols were approved by the Mayo Clinic Institutional Review Board.

We also used OC RNA-seq from TCGA (n=419) and from normal ovarian tissue from the Genotype-Tissue Expression (GTEx) project (Broad Institute) (n=84) [9, 22].

Bioinformatics methods
RNA-seq of Mayo Clinic, TCGA, and GTEx data sequencing reads were processed through the Mayo Clinic MAP-RSeq v.2.1.5 computational workflow, and variants were calculated with RVboost 0.1 [18, 23]. We considered expressed single nucleotide variants from

Table 1 Characteristics of the 195 patients in the Mayo Clinic ovarian cancer cohort

Feature	Value
Age at diagnosis, mean (SD), y	62 (12)
Histology, no. (%)	
Serous	114 (58)
Endometrioid	53 (27)
Clear cell	14 (7)
Undifferentiated	8 (4)
Mucinous	3 (2)
Other	3 (2)
Grade, no. (%)	
1	20 (10)
2	24 (12)
3	146 (75)
Unknown	5 (3)
Stage, no. (%)	
I	45 (23)
II	15 (8)
III	100 (51)
IV	33 (17)
Unknown	2 (1)

Davila *et al. BMC Med Genomics*   (2021) 14:165

Page 3 of 6

RVboost with a Q score greater than 10%, read depth greater than 10, a minor allelic frequency less than 2% in the 1000 Genomes Project [24], and not present in recurrent expressed single-nucleotide variants identified in RNA-seq from adjacent normal tissue. The RNA-seq capture region was defined as positions with $20 \times$ coverage as calculated by the Genome Analysis Toolkit (GATK; Broad Institute). Samples with read depth over $20 \times$ at less than five million positions were excluded from this analysis. Tumor mutation burden (TMB) was calculated as the number of considered expressed variants per capture region $\times 10^6$.

We used the mutational signatures v2 from the Catalogue of Somatic Mutations in Cancer (COSMIC) [25] where the mutational profiles are represented as the proportion of each substitution type (C > A, C > G, C > T, T > A, T > C, and T > G) and its trinucleotide context (the nucleotide before and after each mutated base) [17]. For the detection of mutational signatures and their contribution to each sample, we used R version 3.4.2 (R Foundation) with the MutationalPatterns v1.4.3 package [26]. To measure the similarity between two mutational signatures we used the cosine similarity as implemented in the function *cos_sim* in the MutationalPatterns v1.4.3 package. The cosine similarity takes values between 0 and 1, with a value close to 1 if there is great similarity between signatures and close to 0 if the two signatures are dissimilar.

Statistical analysis

We used R version 3.4.2 with the tidyverse 1.2.1 package to perform statistical analyses and generate graphs. Whiskers in the boxplots correspond 75th (and 25th) Quantile ± 1.5 IQR (Interquantile range) and outliers correspond to values outside this range. Two-sided Mann–Whitney tests (Wilcoxon rank sum tests) were used for comparisons of contributions of *POLE* mutational signature across the Mayo OC cohort and TCGA/GTEx, and age across patients with and without *POLE* mutations. Histology findings from patients with and without *POLE* mutations were compared with the Fisher exact test.

Results

The Mayo Clinic OC cohort with existing RNA-seq consisted of 195 patients whose clinical characteristics are described in Table 1 [20, 21]. This cohort, contains an abundance of nonserous histologies (81 of 195) and includes 53 with OEC, which makes it the largest OEC RNAseq collection to date.

Mutational profiles from eSNV were calculated in the Mayo Clinic OC tumors (n = 195), TCGA OC tumors (n = 419), and the GTEx normal ovarian tissues (n = 84). Using Non-negative Matrix Factorization (NMF) [26]

we were able to approximate each sample's mutational profile as a combination of four distinct mutational signatures (Fig. 1a and Additional file 1: Fig. S1). Using the cosine similarity, we established a high degree of resemblance between the approximated mutational profiles from NMF and the original mutational profile (median cosine similarity, 0.92; interquartile range, 0.89–0.93) (Additional file 1: Fig. S2).

Using the cosine similarity, the four mutational signatures were compared against the COSMIC mutational signatures catalog v2 (Fig. 1b) [17]. Signature B has a cosine similarity of 0.91 against COSMIC signature 1 which is associated with aging [27]. Signature C has cosine similarities of 0.85 and 0.77 against COSMIC signatures 4 and 3, which are associated with tobacco exposure and defective double strand repair respectively [17].
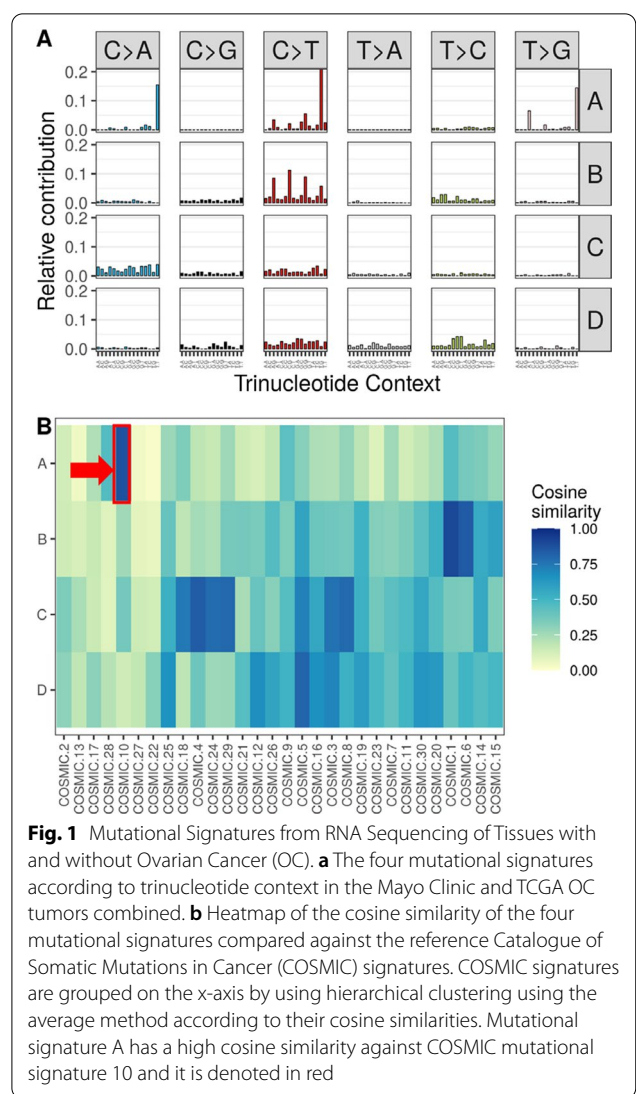
Fig. 1 Mutational Signatures from RNA Sequencing of Tissues with and without Ovarian Cancer (OC). **a** The four mutational signatures according to trinucleotide context in the Mayo Clinic and TCGA OC tumors combined. **b** Heatmap of the cosine similarity of the four mutational signatures compared against the reference Catalogue of Somatic Mutations in Cancer (COSMIC) signatures. COSMIC signatures are grouped on the x-axis by using hierarchical clustering using the average method according to their cosine similarities. Mutational signature A has a high cosine similarity against COSMIC mutational signature 10 and it is denoted in red

Davila *et al. BMC Med Genomics*   (2021) 14:165

Page 4 of 6

Signature D has a cosine similarity of 0.81 against COS-MIC signature 5, a signature found in all cancer types [17].

Of note, signature A has a cosine similarity of 0.88 to COSMIC signature 10, which is associated with *POLE* defects [2]. Six samples in the Mayo Cohort have a similar mutational distribution characterized by an enrichment of the *POLE* contribution (Additional file 1: Fig. S1B and C).
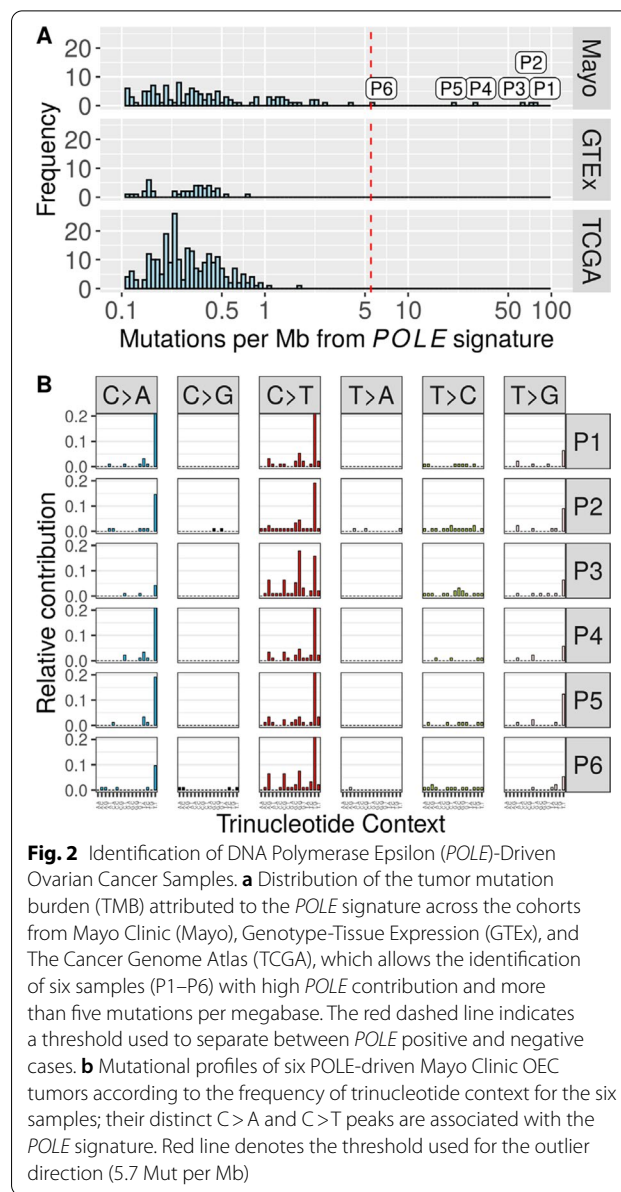
The *POLE* signature contribution of such six samples (of 195) from our Mayo OC were deemed as outliers (> 5.74 Mut per megabase) (see Methods and Additional file 1: Fig. S3). Normal samples from GTEx and serous OC samples from TCGA had a median of 0.16 mutations per megabase; maximum 1.78 mutations per megabase of the *POLE* signature and can be used as negative *POLE* controls (Fig. 2a). The six outlier Mayo OC samples have a higher *POLE* signature contribution (median 46.34 mutations per megabase; $P = 2.37\mathrm{E}{-}05$) when compared to the negative *POLE* controls (Fig. 2a). The individual mutational profiles for each of those six samples are shown in Fig. 2b.

Within these six samples, we found expressed mutations corresponding to the *POLE* hotspot COSMIC mutations *P286R, S297F, V411L,* and *A456P* (Table 2 and on Additional file 1: Fig. S3) [28]. No other samples in the Mayo OC, the TCGA OC, or the normal ovarian GTEx cohort harbored expressed mutations in any of the *POLE* hotspots.

All six samples were of endometrioid histotype ($P = 5\mathrm{e}{-}04$) and constituted 11% of OEC cases. Average age at onset was earlier (48.33 years) than in the non-*POLE* OEC cohort (60.13 years; $P = 0.008$). Four of these six samples corresponded to stage 1, and two corresponded to stage 3 (Table 2).

Discussion

RNA-seq is routinely used for transcriptome quantification and fusion detection, as illustrated by our previous studies where we characterized gene expression and fusions across different OC histology types [20, 21]. This study constitutes a novel reuse of this OC RNA-seq cohort, along with multiple public RNA-seq datasets including TCGA and GTEx, to enable clinically significant discoveries of previously unidentified *POLE* altered cases. Furthermore, our bioinformatics approach can identify the distinct *POLE* mutational signatures in RNA-seq as well as confirm the expression of *POLE* hotspot mutations. This adds to the clinical utility of RNA-seq which can already detect fusions and calculate tumor mutational burden in a single clinical assay, as opposed to DNA-seq [29, 30].

Fig. 2 Identification of DNA Polymerase Epsilon (*POLE*)-Driven Ovarian Cancer Samples. **a** Distribution of the tumor mutation burden (TMB) attributed to the *POLE* signature across the cohorts from Mayo Clinic (Mayo), Genotype-Tissue Expression (GTEx), and The Cancer Genome Atlas (TCGA), which allows the identification of six samples (P1–P6) with high *POLE* contribution and more than five mutations per megabase. The red dashed line indicates a threshold used to separate between *POLE* positive and negative cases. **b** Mutational profiles of six POLE-driven Mayo Clinic OEC tumors according to the frequency of trinucleotide context for the six samples; their distinct C > A and C > T peaks are associated with the *POLE* signature. Red line denotes the threshold used for the outlier direction (5.7 Mut per Mb)

POLE-driven tumors have a favorable prognosis, an increased number of tumor-infiltrating lymphocytes, and can benefit from immunotherapy. Despite these distinct characteristics of *POLE*-driven tumors, *POLE* mutation status is not routinely evaluated in a clinical setting for OEC. By using RNA-seq on the largest OEC cohort to our knowledge (n = 53), we found six of 53 OEC samples (11%) that were *POLE*-driven. Those six samples had a highly specific mutational profile corresponding to the well-characterized *POLE* COSMIC signature 10 profile, and *POLE* hotspot mutations (*P286R, S297F, V411L,* and *A456P*). Two of the 6 patients in the group of *POLE* cases had advanced-stage OEC with relatively high recurrence

Davila *et al. BMC Med Genomics*   (2021) 14:165

Page 5 of 6

Table 2 Clinical Characteristics of six *POLE* Samples from the Mayo Clinic Ovarian Cancer Cohort

Sample	*POLE* mutation	*POLE* TMB	Age, years	Histology	Stage	Grade	Vital status
P1	A456P	75.2	46	Endometrioid	III	2	Alive
P2	S297F	71.7	49	Endometrioid	I	3	Alive
P3	V411L	64.1	49	Endometrioid	III	3	Deceased
P4	P286R	28.6	46	Endometrioid	I	2	Alive
P5	P286R	21.6	49	Endometrioid	I	1	Alive
P6	V411L	5.8	51	Endometrioid	I	1	Alive

POLE DNA polymerase epsilon, *TMB* tumor mutation burden

risks; therefore, OEC patients with *POLE*-driven tumors can be eligible for immunotherapy trials if their cancers progress or recur.

The tumor mutational burden (TMB) attributed to COSMIC signature 10 of our *POLE* cases spans from over five to more than 75 mutations per megabase. Patients with higher TMB attributed to COSMIC signature 10 have worse clinical characteristics and outcomes than among non-POLE OECs; the sample with the lowest TMB was from a patient with a low-grade, stage 1 cancer, and the three samples with the highest TMB correspond to higher-grade or higher stage cancers. However, the limited number of *POLE* cases in this study precluded any statistical analysis, and further independent studies with larger sample sizes are necessary to validate and confirm such a trend.

The smaller number of mutations in RNA-seq as compared to Whole Genomic Sequencing (WGS) reduces the statistical power to find known signatures present at lower levels and to distinguish the contribution of closely related and flat signatures. To illustrate this point, COSMIC signature 3 which is associated with defective homologous recombination and is prevalent in OC had only cosine similarity of 0.77 against signature C, while signature 4 which is associated with tobacco and not known to play a role in OC had a cosine similarity of 0.84 against signature C. Future studies to quantify the limit of detection of mutational signatures in RNA-seq are warranted.

Conclusions

Using RNA-seq mutational signatures from the largest OEC cohort to date (n = 53), we found that 6 hypermutated samples (11%) had evidence of *POLE*-driven tumors.

Abbreviations

COSMIC: Catalogue of Somatic Mutations in Cancer; GTEx: Genotype-Tissue Expression; MMR: mismatch repair; MSK-IMPACT: Memorial Sloan Kettering integrated mutation profiling of actionable cancer targets; OC: ovarian cancer; OEC: ovarian endometrioid cancer; POLE: DNA polymerase epsilon; RNA-seq: RNA sequencing; TCGA: The Cancer Genome Atlas; TMB: tumor mutation burden.

Supplementary Information

Additional file 1. Supplementary Figures.

Availability of data and materials
The datasets and code generated during and/or analyzed during the current study are available in https://github.com/jdavilal/mutational_sig_oec.

Declarations

Ethics approval and consent to participate
All patients gave informed consent, and all protocols were approved by the Mayo Clinic Institutional Review Board. All methods were carried out in accordance with relevant guidelines and regulations.

Consent for publication
Consent for publication is not applicable.

Competing interests
The authors declare that they have no competing interests.

Author details
[1]Department of Mathematics, Statistics and Computer Science, St Olaf College, Northfield, MN, USA. [2]Department of Health Sciences Research, Mayo Clinic, Rochester, MN, USA. [3]Division of Shared Resources, Fred Hutchinson Cancer Research Center, Seattle, WA, USA. [4]Division of Medical Oncology, Mayo Clinic, Rochester, MN, USA. [5]Division of Anatomic Pathology, Mayo Clinic, Rochester, MN, USA.

Davila *et al. BMC Med Genomics*   (2021) 14:165

Page 6 of 6

References

1. Pursell ZF, Isoz I, Lundström E-B, Johansson E, Kunkel TA. Yeast DNA polymerase epsilon participates in leading-strand DNA replication. Science. 2007;317(5834):127–30.
2. Cancer Genome Atlas Network. Comprehensive molecular characterization of human colon and rectal cancer. Nature. 2012;487(7407):330–7.
3. Kandoth C, Schultz N, Cherniack AD, Akbani R, Liu Y, Shen H, et al. Integrated genomic characterization of endometrial carcinoma. Nature. 2013;497(7447):67–73.
4. Shinbrot E, Henninger EE, Weinhold N, Covington KR, Göksenin AY, Schultz N, et al. Exonuclease mutations in DNA polymerase epsilon reveal replication strand specific mutation patterns and human origins of replication. Genome Res. 2014;24(11):1740–50.
5. Rayner E, van Gool IC, Palles C, Kearsey SE, Bosse T, Tomlinson I, et al. A panoply of errors: polymerase proofreading domain mutations in cancer. Nat Rev Cancer. 2016;16(2):71–81.
6. Church DN, Stelloo E, Nout RA, Valtcheva N, Depreeuw J, ter Haar N, et al. Prognostic significance of POLE proofreading mutations in endometrial cancer. J Natl Cancer Inst. 2015;107(1):402.
7. Howitt BE, Shukla SA, Sholl LM, Ritterhouse LL, Watkins JC, Rodig S, et al. Association of polymerase e-mutated and microsatellite-instable endometrial cancers with neoantigen load, number of tumor-infiltrating lymphocytes, and expression of PD-1 and PD-L1. JAMA Oncol. 2015;1(9):1319–23.
8. Mehnert JM, Panda A, Zhong H, Hirshfield K, Damare S, Lane K, et al. Immune activation and response to pembrolizumab in POLE-mutant endometrial cancer. J Clin Invest. 2016;126(6):2334–40.
9. Cancer Genome Atlas Research Network. Integrated genomic analyses of ovarian carcinoma. Nature. 2011;474(7353):609–15.
10. Zou Y, Liu FY, Liu H, Wang F, Li W, Huang MZ, et al. Frequent POLE1 p.S297F mutation in Chinese patients with ovarian endometrioid carcinoma. Mutat Res. 2014;761:49–52.
11. Hoang LN, McConechy MK, Köbel M, Anglesio M, Senz J, Maassen M, et al. Polymerase epsilon exonuclease domain mutations in ovarian endometrioid carcinoma. Int J Gynecol Cancer. 2015;25(7):1187–93.
12. Cybulska P, Paula ADC, Tseng J, Leitao MM Jr, Bashashati A, Huntsman DG, et al. Molecular profiling and molecular classification of endometrioid ovarian carcinomas. Gynecol Oncol. 2019;154(3):516–23.
13. Ishikawa M, Nakayama K, Nakamura K, Ono R, Yamashita H, Ishibashi T, et al. High frequency of POLE mutations in synchronous endometrial and ovarian carcinoma. Hum Pathol. 2019;85:92–100.
14. Leskela S, Romero I, Rosa-Rosa JM, Caniego-Casas T, Cristobal E, Pérez-Mies B, et al. Molecular heterogeneity of endometrioid ovarian carcinoma: an analysis of 166 cases using the endometrial cancer subrogate molecular classification. Am J Surg Pathol. 2020;44(7):982–90.
15. Parra-Herran C, Lerner-Ellis J, Xu B, Khalouei S, Bassiouny D, Cesari M, et al. Molecular-based classification algorithm for endometrial carcinoma categorizes ovarian endometrioid carcinoma into prognostically significant groups. Mod Pathol. 2017;30(12):1748–59.
16. Teer JK, Yoder S, Gjyshi A, Nicosia SV, Zhang C, Monteiro ANA. Mutational heterogeneity in non-serous ovarian cancers. Sci Rep. 2017;7(1):9728.
17. Alexandrov LB, Nik-Zainal S, Wedge DC, Aparicio SA, Behjati S, Biankin AV, et al. Signatures of mutational processes in human cancer. Nature. 2013;500(7463):415–21.
18. Wang C, Davila JI, Baheti S, Bhagwate AV, Wang X, Kocher JP, et al. RVboost: RNA-seq variants prioritization using a boosting method. Bioinformatics. 2014;30(23):3414–6.
19. Jessen E, Liu Y, Davila J, Kocher J-P, Wang C. Determining mutational burden and signature using RNA-seq from tumor-only samples. BMC Med Genomics. 2021;14(1):65.
20. Earp MA, Raghavan R, Li Q, Dai J, Winham SJ, Cunningham JM, et al. Characterization of fusion genes in common and rare epithelial ovarian cancer histologic subtypes. Oncotarget. 2017;8(29):46891–9.
21. Fridley BL, Dai J, Raghavan R, Li Q, Winham SJ, Hou X, et al. Transcriptomic characterization of endometrioid, clear cell, and high-grade serous epithelial ovarian carcinoma. Cancer Epidemiol Biomark Prev. 2018;27(9):1101.
22. Lonsdale J, Thomas J, Salvatore M, et al. The Genotype-Tissue Expression (GTEx) project. Nat Genet. 2013;45(6):580–5.
23. Kalari KR, Nair AA, Bhavsar JD, O'Brien DR, Davila JI, Bockol MA, et al. MAP-RSeq: mayo analysis pipeline for RNA sequencing. BMC Bioinform. 2014;15:224.
24. Auton A, Brooks LD, Durbin RM, Garrison EP, Kang HM, Korbel JO, et al. A global reference for human genetic variation. Nature. 2015;526(7571):68–74.
25. Tate JG, Bamford S, Jubb HC, Sondka Z, Beare DM, Bindal N, et al. COSMIC: the catalogue of somatic mutations in cancer. Nucl Acids Res. 2019;47(D1):D941–7.
26. Blokzijl F, Janssen R, van Boxtel R, Cuppen E. MutationalPatterns: comprehensive genome-wide analysis of mutational processes. Genome Med. 2018;10(1):33.
27. Alexandrov LB, Jones PH, Wedge DC, Sale JE, Campbell PJ, Nik-Zainal S, et al. Clock-like mutational processes in human somatic cells. Nat Genet. 2015;47(12):1402–7.
28. Tate JG, Bamford S, Jubb HC, Sondka Z, Beare DM, Bindal N, et al. COSMIC: the catalogue of somatic mutations in cancer. Nucl Acids Res. 2018;47(D1):D941–7.
29. Winters JL, Davila JI, McDonald AM, Nair AA, Fadra N, Wehrs RN, et al. Development and verification of an RNA sequencing (RNA-Seq) assay for the detection of gene fusions in tumors. J Mol Diagn. 2018;20(4):495–511.
30. DiGuardo MA, Davila JI, Jackson RA, Nair AA, Fadra N, Minn KT, et al. RNA-Seq reveals differences in expressed tumor mutation burden in colorectal and endometrial cancers with and without defective DNA-mismatch repair. J Mol Diagn. 2021;23(5):555–64.

Publisher's Note